Hydrothermal Synthesis, Crystal Structures, and Properties of a Class of 2D Coordination Polymers

Xiang He,[a] Can-Zhong Lu*[a] Da-Qiang Yuan,[a] Li-Juan Chen,[a] Quan-Zheng Zhang,[a] and Chuan-De Wu[a]

Keywords: Coordination polymers / Copper / Magnetic properties / Photoluminescence / Zinc

Hydrothermal reactions between 2,6-naphthalenedicarboxylic acid (H_2NDC), 1,10-phenanthroline (1,10-phen) or 2,2′-bipyridine (2,2′-bpy), and transition metal acetates give rise to four coordination polymers, namely $[Cu_3(NDC)_3(2,2'\text{-bpy})(H_2O)_2]_n\cdot nH_2O$ (**1**), $[Cu(NDC)(1,10\text{-phen})]_n$ (**2**), $[Zn(NDC)(1,10\text{-phen})]_n$ (**3**), and $[Zn_4(OH)_2(NDC)_3(2,2'\text{-bpy})_2]_n$ (**4**), which show different two-dimensional layered architectures. Compound **1** consists of three kinds of polymeric chains that are interconnected to form an unusual two-dimensional layered motif, while compound **4** features a two-dimensional honeycomb network structure with a noninterpenetrating ABCDABCD packing pattern. Compounds **2** and **3** show a two-dimensional grid-type framework but have different space-filling styles. The magnetic properties for **1** and **2** and the solid-state emission spectra of **3** and **4** have also been studied.

Introduction

The construction of extended porous metal–organic frameworks (MOFs) is of current interest in the fields of supramolecular chemistry and crystal engineering, not only because of their intriguing architectures but also because of their unexpected properties for potential practical applications in a wide number of fields, such as gas storage, exploitable magnetics, photoluminescence, and molecular recognition.[1–4] The self-assembly of MOFs using suitable ligands and metal centers has been proved to be an efficient route for the formation of one- to three-dimensional networks with fascinating structural topologies. The selection of organic ligands with appropriate coordination sites is the key to the formation of MOFs with desirable physical and chemical properties. Recently, the strategy using metal ions and organic carboxylates as starting building blocks to generate extended networks has been of great interest.[5–14] For example, 1,4-benzenedicarboxylate-(BDC-)bridged metal-organic frameworks have been studied extensively.[15] Polycyclic aromatic bidentate ligands such as 2,2′-bipyridine and 1,10-phenanthroline are frequently used together with polycarboxylates, leading to many novel architectures. Most of the coordination polymers with BDC and 2,2′-bipyridine or 1,10-phenanthroline ligands are often one-dimensional structures.[16] We are currently interested in employing 2,6-naphthalenedicarboxylate (NDC) as a bridging ligand since this molecule is more rigid than BDC and might not only establish bridges between several metal centers and exhibit rich coordination modes but also be expected to form a porous framework because of its rigidity and stability. On the other hand, because the presence of conjugated aromatic rings causes its low solubility in aqueous media, quite a few examples of polymeric structures containing both NDC and other multipyridine ligands have been reported.[17]

In the present work, we have selected Cu^{II} and Zn^{II} cations as metal nodes and NDC as a rigid bridging ligand and obtained four interesting 2D polymeric compounds, namely $[Cu_3(NDC)_3(2,2'\text{-bpy})(H_2O)_2]_n\cdot nH_2O$ (**1**), $[Cu(NDC)(1,10\text{-phen})]_n$ (**2**), $[Zn(NDC)(1,10\text{-phen})]_n$ (**3**), and $[Zn_4(OH)_2(NDC)_3(2,2'\text{-bpy})_2]_n$ (**4**). Compound **1** consists of three different chains that are interconnected to form an unusual two-dimensional layered motif, while compound **4** features a two-dimensional honeycomb network structure with a noninterpenetrating ABCDABCD packing pattern. Compounds **2** and **3** show a two-dimensional grid-type framework but have different space-filling styles.

Results and Discussion

Synthesis

Although it is difficult to control and predict the crystal structures under hydrothermal conditions, the hydrothermal reaction is still an optimum method for the synthesis of some novel MOFs. We used Cu^{II} and Zn^{II} salts and mixed bridging ligands to obtain four 2D compounds with distinct structures under hydrothermal conditions. Subtle adjust-

---

[a] State Key Laboratory of Structural Chemistry, Fujian Institute of Research on the Structure of Matter, The Chinese Academy of Sciences,
Fuzhou, Fujian, 350002, China
Fax: +86-591-8371-4946
E-mail: czlu@ms.fjirsm.ac.cn

DOI: 10.1002/ejic.200500490

ments of the conditions result in the formation of very different structures.

Crystal Structures

[$Cu_3(NDC)_3(2,2'\text{-}bpy)(H_2O)_2]_n\cdot nH_2O$ (1)

Compound **1** consists of three different chains that are interconnected to form an unusual two-dimensional layered motif – one is a zigzag chain and the other two are linear chains. The NDC ligands in the zigzag chain act as the junctions to link the two linear chains into a layered structure. As shown in Figure 1, the asymmetric unit contains two crystallographically unique Cu centers. Each Cu^{II} center has a quite different coordination environment: the first one has a $\{CuO_2N_2\}$ coordination sphere and is coordinated by two nitrogen atoms from one 2,2′-bpy [Cu–N = 1.984(6) Å] and two oxygen atoms from two NDC ligands [Cu–O = 1.966(5) Å] with O(N)–Cu–O(N) angles involving the neighboring atoms ranging from 82.5(2) to 97.7(2)°, showing a disordered square-planar structure, and the second one has a $\{CuO_4\}$ square-planar coordination sphere and is defined by three oxygen donors from three individual NDC ligands [Cu–O = 1.932(5)–1.996(5) Å] and one from a water molecule [Cu–O = 1.969(6) Å]. The trinuclear copper unit formed can be taken as an isosceles triangular array linked by the NDC ligands. The NDC ligands in compound **1** exhibit two different coordination modes (Scheme 1): one (NDC with O5) acts as a tetradentate ligand to link four copper(II) centers (mode I), while another (NDC with O1) acts as a bidentate ligand connecting two copper(II) centers in an *anti* fashion (mode II). As shown in Figure 2, the bidentate carboxyl groups bridge the Cu(2) atom to form linear chains running alone the *b*-axis, which are parallel to each other. The tetradentate carboxyl groups bridge the Cu(1) atom to form zigzag chains running along the *c*-axis, which also link the neighboring copper atoms in

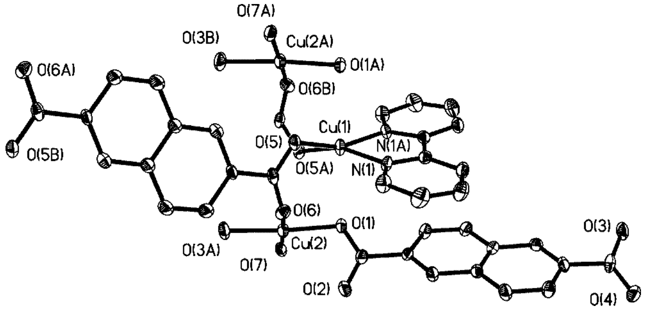

Figure 1. ORTEP representation of the symmetry-expanded structure of **1**, showing the coordination environments of the Cu^{II} atoms (30% probability thermal ellipsoids; hydrogen atoms and solvent molecules have been omitted for clarity).

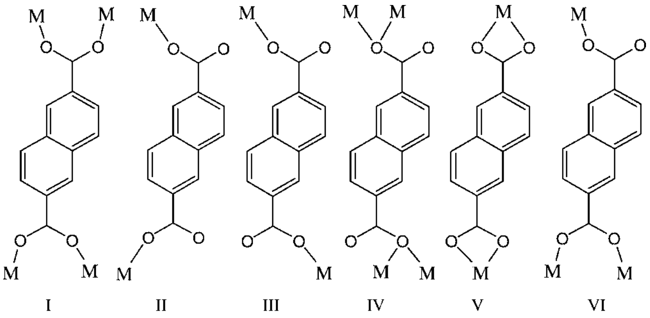

Scheme 1. Different kinds of coordination modes of the NDC ligand.

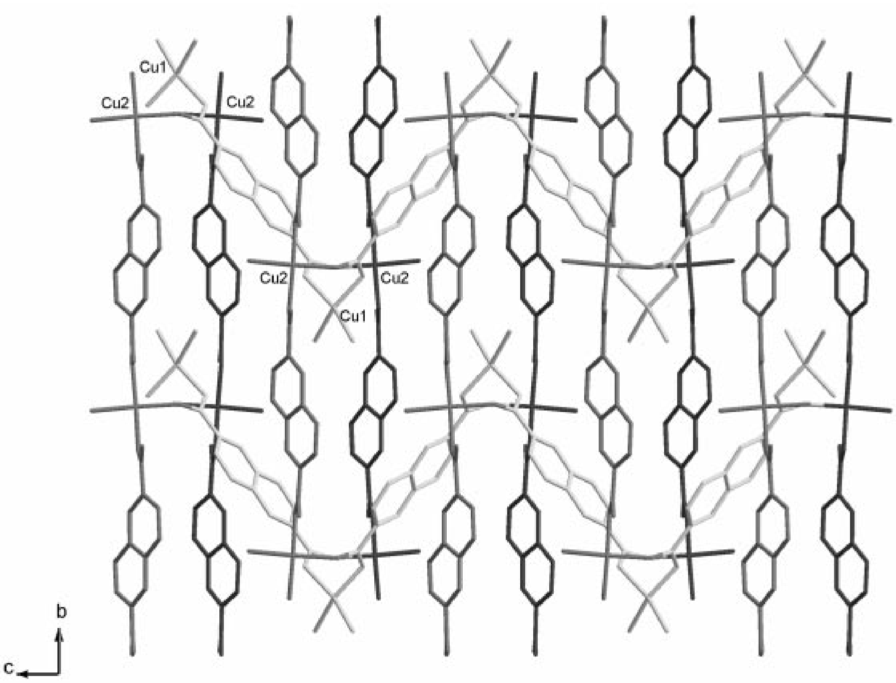

Figure 2. Perspective view of the 2D layer structure of **1**.

linear chains to form a thick, trilayer network. Each zigzag chain is parallel to the others, while the linear chains located behind and ahead of the zigzag chain are parallel to each other too.

The Cu···Cu distance within the zigzag chain bridged by the NDC ligand is 13.022(1) Å, while the Cu···Cu distance is 13.006(1) Å in the linear chain. The Cu···Cu distance between two neighboring linear chains is 5.638(8) Å, and the Cu···Cu distance between zigzag and linear chains is 3.395(3) Å. It is notable that the lamellar framework is made up by zigzag chains sandwiched between two adjacent linear chains. To the best of our knowledge, no documented example of such a layered structure has been reported.

[Cu(NDC)(1,10-phen)]$_n$ (2)

Compound **2** is a two-dimensional, square-grid network structure. As shown in Figure 3, the copper(II) atom exhibits a square-pyramidal configuration, coordinated by two nitrogen atoms of one 1,10-phen ligand [Cu–N = 2.029(2)–2.050(2) Å] and three oxygen atoms of the carboxyl groups from different NDC ligands [Cu–O = 1.9139(18)–2.2421(17) Å]. The O–Cu–O bond angles range from 95.89(8) to 102.41(7)° and the O–Cu–N bond angles range from 90.52(8) to 170.58(8)°. The NDC ligands in compound **2** exhibit two different coordination modes (Scheme 1): one (NDC with O3) acts as a tetradentate ligand to link four copper(II) centers (mode I), while another (NDC with O1) acts as a bidentate ligand that connects two copper(II) centers in a *trans* fashion (mode III). As shown in Figure 4a, the carboxylate groups at both ends of the NDC ligands doubly bridge the Cu dimers with a Cu···Cu separation of 4.319(3) Å to yield an infinite chain running along the *a*-axis, in which the four carboxylate oxygen atoms and two Cu atoms form an O_4Cu_2 six-membered ring. The 1D chains are stitched by the bis(monodentate) bridges along the *b*-axis to form a 2D square-grid coordination polymer with dimensions of 13.801(1) × 12.082(1) Å^2, of which the effective pore-size is partly diminished by the phen ligands. Calculations with PLATON show that the pores occupy about 47.0% of the crystal volume. Intramolecular nonclassical weak hydrogen-bonding interactions between the carbon atoms of the 1,10-phen ligand and the oxygen atoms of the carboxylate groups C(10)–H(10A)··· O(4) (–*x*, –*y*, –*z*) [3.063(3) Å] exist in compound **2**. In addition, there are π–π stacking interactions between adjacent aromatic rings of phen ligands, with a plane-to-plane separation of about 3.528 Å in **2**.

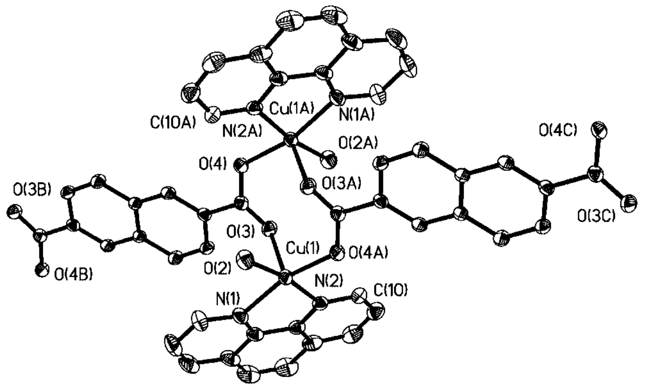

Figure 3. ORTEP representation of the symmetry-expanded structure of **2**, showing the coordination environments of the Cu^{II} atoms (30% probability thermal ellipsoids; hydrogen atoms have been omitted for clarity).

[Zn(NDC)(1,10-phen)]$_n$ (3)

The structure of **3** is also a two-dimensional square-grid network. As shown in Figure 5, the zinc(II) atom exhibits a distorted octahedral configuration, coordinated by two nitrogen atoms of a 1,10-phen ligand [Zn–N = 2.109(6)–2.173(7) Å] and four oxygen atoms of the carboxyl groups from different NDC ligands. The Zn–O distances range from 2.074(5) to 2.177(5) Å, the O–Zn–O bond angles range from 60.8(2) to 155.1(2)°, and the O–Zn–N bond angles range from 90.8(2) to 169.5(2)°. The NDC ligands in compound **3** also exhibit two different coordination modes (Scheme 1): one (NDC with O4) acts as a tetradentate ligand to link four zinc(II) atoms by two carboxylate oxygen atoms on two side (mode IV), while another (NDC with O1) bidentate NDC ligand chelates two zinc(II) centers

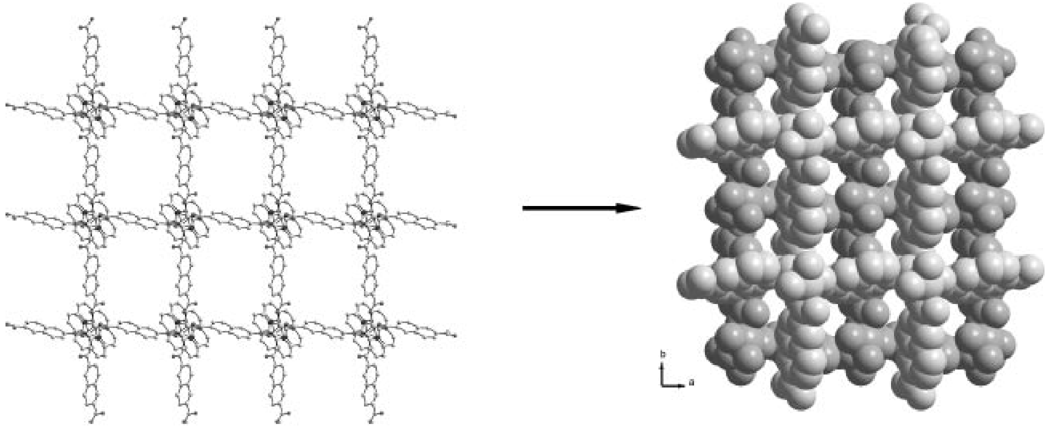

Figure 4. a) Structure of **2**, showing the 2D square grid. b) Space-filling representation of the stacking of 2D layers in **2**.

(mode V). As shown in Figure 6a, the carboxylate groups at both ends of the NDC ligands doubly bridge Zn dimers with a Zn···Zn separation of 3.207(2) Å to yield an infinite chain in which the two carboxylate oxygen atoms and two Zn atoms form O_2Zn_2 four-membered rings. These chains are stitched by the bis(bidentate) bridges to give a 2D layer architecture. It is interesting to note that the adjacent layers possess large channels with approximate dimensions of 12.899(7) × 11.147(10) Å^2, with the phen ligands inserted inside such grids. Calculations with PLATON show that the pores occupy about 39.2% of the crystal volume. Intramolecular nonclassical weak hydrogen-bonding interactions between the carbon atoms of the 1,10-phen ligand and the oxygen atoms of the carboxylate groups C(1)–H(1A)···O(3) ($-x + 1$, $-y + 1$, $-z + 2$) [3.281(12) Å] also exist in compound **3**. In addition, there are π–π stacking interactions between adjacent aromatic rings of the phen ligands, with a plane-to-plane separation of about 3.568 Å in **3**.

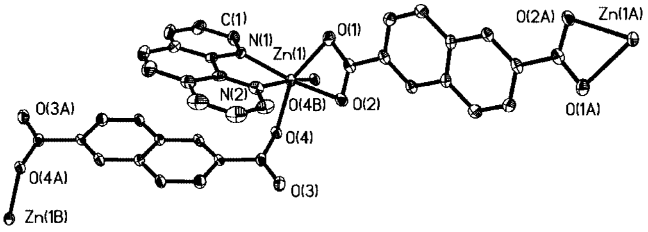

Figure 5. ORTEP representation of the symmetry-expanded structure in **3**, showing the coordination environments of the Zn^{II} atoms (30% probability thermal ellipsoids; hydrogen atoms have been omitted for clarity).

Comparing the different space-filling styles between compounds **2** and **3**, we find that the phen ligands fill the grids, resulting in the different space-filling frameworks. In compound **2**, the phen ligands align above and below one sheet and protrude into the cavities of neighboring networks. Two adjacent square grids are stacked parallel but in a staggered manner to each other along the *c*-direction. This arrangement ultimately leads to an ABAB repeat pattern of layers (Figure 4b). The phen ligands are inserted into the square grids like guest molecules in compound **3**, leading to an AA stacking pattern in the *bc* plane (Figure 6b).

[Zn$_4$(OH)$_2$(NDC)$_3$(2,2′-bpy)$_2$]$_n$ (4)

Compound **4** is a two-dimensional honeycomb network structure with a Zn_2O core as building block that is bridged by a hydroxy group. As shown in Figure 7, the Zn^{II} atoms comprise two different coordination environments: Zn(1) is coordinated by four oxygen atoms in a disordered tetrahedral geometry, with three oxygen donors from individual NDC ligands [Zn(1)–O = 1.932(2)–2.005(2) Å] and one from a hydroxy group [Zn(1)–O = 1.918(2) Å], while Zn(2) is five-coordinated by two 2,2′-bpy nitrogen atoms [Zn(2)–N = 2.078(5)–2.203(6) Å], two oxygen atoms of NDC ligands [Zn(2)–O = 2.028(2)–2.065(3) Å], and one hydroxy group [Zn(2)–O(5) = 1.918(2) Å] to furnish a square-pyramidally coordinated environment. The carboxylate groups exhibit two different coordinating modes (Scheme 1): one (NDC with O1) acts as a tridentate ligand to link three zinc(II) centers (mode VI), while another (NDC with O3)

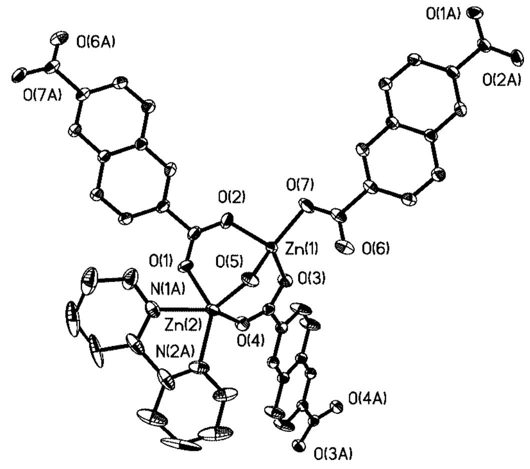

Figure 7. ORTEP representation of the symmetry-expanded structure of compound **4**, showing the coordination environments of the Zn^{II} atoms (30% probability thermal ellipsoids; hydrogen atoms and one disordered bipy have been omitted for clarity).

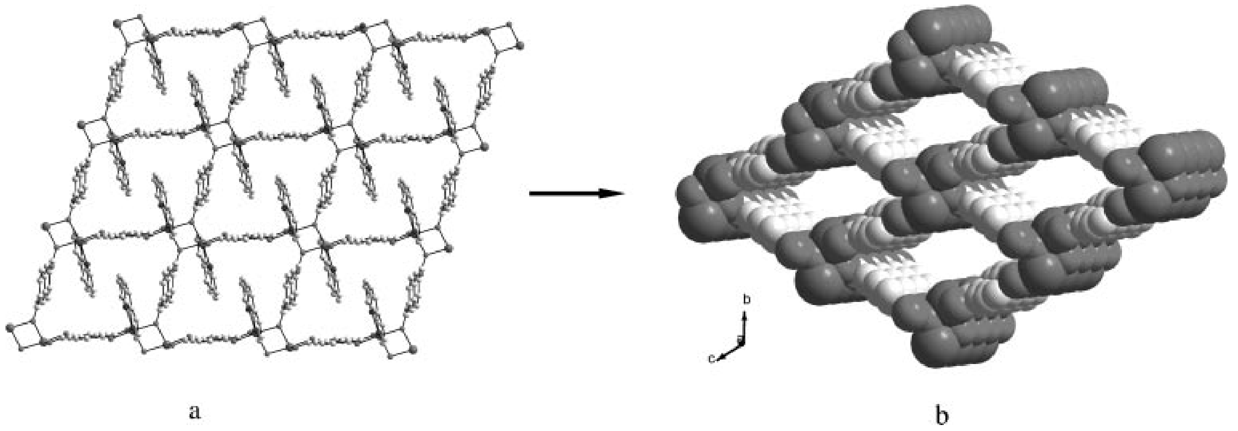

Figure 6. a) Structure of **3**, showing the 2D square grid. b) Space-filling representation of the 2D nanosized channels (2,2′-bpy ligands omitted) in **3**.

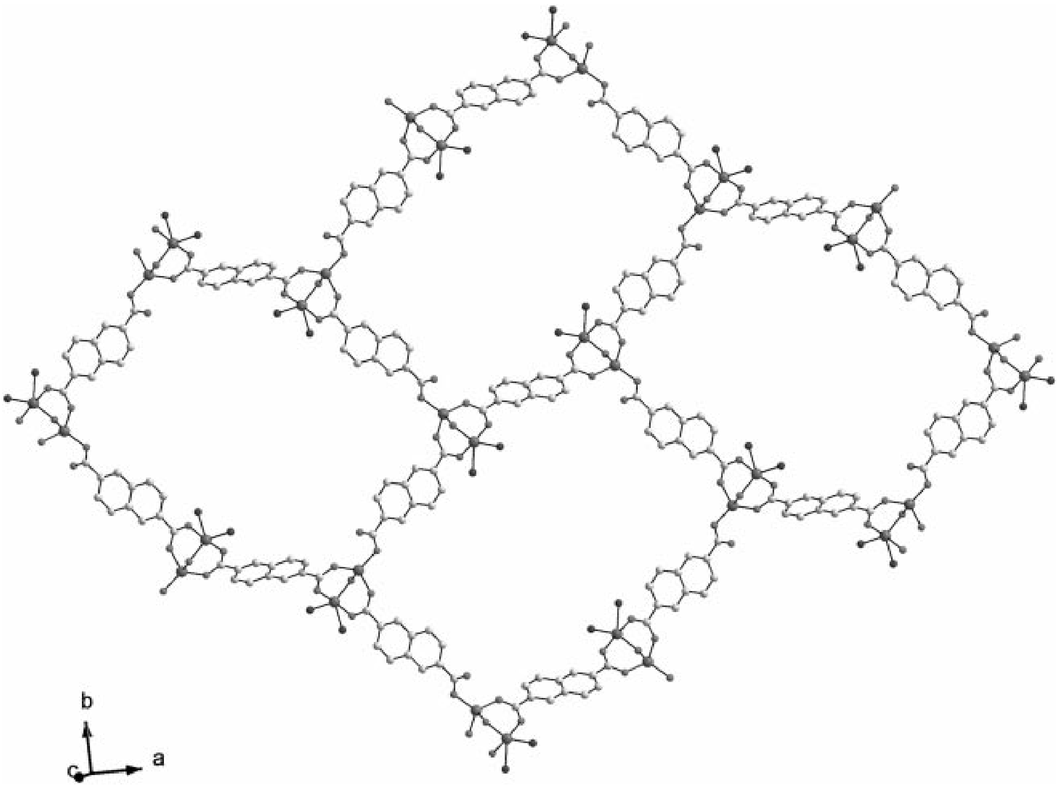

Figure 8. View of the 2D hexagonal grid (2,2′-bpy ligands omitted) of compound **4**.

acts as a tetradentate ligand to link four zinc(II) centers (mode I).

The Zn_2O building units are bridged by four tridentate and two tetradentate NDC ligands to form a hexagon with dimensions of 18.9×26.1 Å^2 (Figure 8). To the best of our knowledge, the simultaneous presence of two coordination modes of NDC ligands to form a hexagon has not been reported until now. Each hexagon shares six edges with six adjacent hexagons to form a 2D framework. It is noteworthy that the topology of compound **4** can be simplified as a (6,3) network.

Other examples of honeycomb compounds often form interpenetrated networks – one 3D fourfold interpenetrated[18] and one 2D twofold interpenetrated[19] supramolecular architectures have been reported. In contrast, compound **4** is an unusual example of a 2D noninterpenetrated honeycomb structure in which these 2D honeycomb networks are stacked together in an ABCDABCD packing mode along the *c*-axis (Figure 9), which is different to that of the other reported noninterpenetrated networks.[20,21] To the best our knowledge, compound **4** is the first example of a 2D noninterpenetrated honeycomb structure with an ABCDABCD packing pattern.

The NDC ligands possess rich coordination modes in the above four 2D structures, which results in the formation of four interesting compounds. The aromatic and rigid part of naphthalene may help the growth of high-quality crystals. Polycyclic N-heterocyclic ligands such as 2,2′-bipyridine or 1,10-phenanthroline might affect the structures due to steric factors. Finally, the different metal cations may also play important roles in the synthesis of novel multidimensional open-framework materials due to their intrinsic ability to form diverse geometric structures.

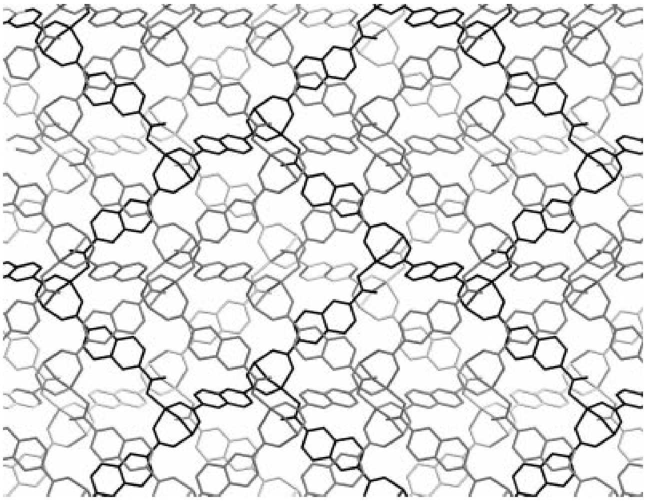

Figure 9. View of the stacking of sheets along the *c*-axis of compound **4** (different shades of gray represent distinct sheets).

Thermogravimetric Analysis

To study the thermal stabilities of these polymers, the thermogravimetric analyses (TGA) of compounds **2**–**4** were performed. The TGA diagram of **2** shows two main weight-loss steps. From 30 to 260 °C compound **2** is stable. In the temperature range of 260–327 °C, the observed weight loss of 39.11% is attributed to the elimination of the phen ligands (calcd. 39.35%). The second step is attributed to the further decomposition of NDC ligands. The TGA diagram of **3** is similar to that of **2**, as compound **3** is stable up to 385 °C. In the temperature range of 385–444 °C, the weight loss of 39.21% is attributed to the elimination of phen ligands (calcd. 39.20%). The next step is attributed to the further decomposition of the NDC ligands. The TGA diagram of **4** also indicates two main weight-loss steps. The observed weight loss of 25.54% (322–412 °C) is attributed to the elimination of bpy ligands (calcd. 24.98%), while the second step is attributed to the further decomposition of NDC ligands and the hydroxy group. The stabilities of **3** and **4** make them potential candidates for practical applications.

Magnetic Properties

The magnetic susceptibilities, χ_M, of compound **1** were measured between 5 and 300 K in a 5 kOe applied magnetic field and all data were corrected for diamagnetism of the ligands estimated from Pascal's constants.[22] The plots of μ_{eff} and χ_M vs. T of compound **1** are shown in Figure 10. The μ_{eff} value is 3.28 μ_B at room temperature, which slightly exceeds the value expected for three independent copper(II) ions (3.00 μ_B). The value of μ_{eff} decreases upon cooling, reaching a value of 2.07 μ_B at 5 K. A number of trinuclear copper compounds have been reported and classified from a structural point of view as linear,[23] isosceles triangle,[24] equilateral triangle,[25] and angular trinuclear.[26] The trinuclear copper center in compound **1** can be taken as an isosceles triangle array, therefore an equation that uses two different J values was tried. In this case, the exchange Hamiltonian takes on the form $H = -2J_1(S_1S_2 + S_1S_3) - 2J_2S_2S_3$. As can be seen from the crystal structure of **1**, there is no magnetic exchange interaction between atoms Cu2 and Cu2A, and therefore we can ignore this interaction ($J_2 = 0$) (Scheme 2). The corresponding molar magnetic susceptibility is expressed by Equation (1), in which a Weiss-like parameter was considered. The symbols in that equation have their usual meaning. It is assumed that the g values for all three copper atoms are equal.

$$\chi_M = \frac{Ng^2\beta^2[15\exp(J_1/KT) + 3/2\exp(-2J_1/KT) + 3/2]}{3k(T-\theta)[4\exp(J_1/kT) + 2\exp(-2J_1/KT) + 2]} \qquad (1)$$

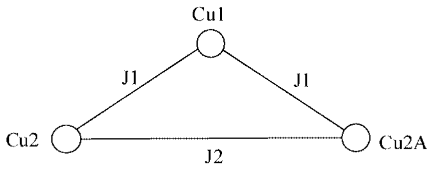

Scheme 2. Different J values for compound **1**.

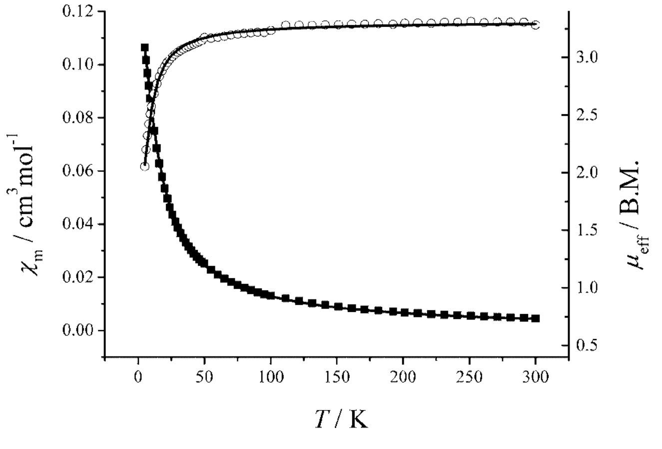

Figure 10. Temperature-dependent experimental molar susceptibility (χ_M) and effective magnetic moment (μ_{eff}) of compound **1**. The solid lines represent the calculated values.

A satisfactory least-squares fitting of the observed data at 5–300 K leads to $g = 2.20$, $J_1 = -4.36$ cm^{-1}, $J_2 = 0$, and $\theta = 0.04$ K with the agreement factor $R = \Sigma(\chi_{M_{obs}} - \chi_{M_{calcd.}})^2/\Sigma(\chi_{M_{obs}})^2 = 8.37 \times 10^{-7}$. The value of J_1 indicates that an antiferromagnetic Cu1···Cu2 exchange interaction occurs through the bridging carboxylate groups of the NDC ligand, while the θ value indicates very weak ferromagnetic interactions between the trinuclear units through the tetradentate bridging carboxylate groups of the NDC ligand.

From the plots of μ_{eff} and χ_M vs. T of **2** (Figure 11), it can be seen that the μ_{eff} value at room temperature is 1.64 μ_B, which is close to the spin-only value of 1.73 μ_B for the Cu^{II} center ($S = 1/2$). To quantitatively interpret the magnetic behavior of the compound, its magnetic data were analyzed by the theoretical expression by using the HDDV model ($H = -2J_1S_1S_2$). The corresponding molar magnetic susceptibility is expressed by Equation (2), in which a Weiss-like parameter was considered. The symbols in this equation have their usual meaning.

$$\chi_M = \frac{Ng^2\beta^2}{k(T-\theta)[3 + \exp(-2J/kT)]} \qquad (2)$$

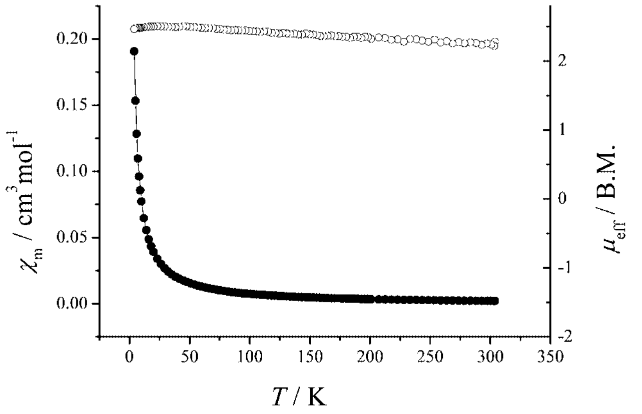

Figure 11. Temperature-dependent experimental molar susceptibility (χ_M) and effective magnetic moment (μ_{eff}) of compound **2**. The solid lines represent the calculated values.

A satisfactory least-squares fitting of the observed data at 5–300 K leads to $g = 2.02$, $J = -2.04$, and $\theta = 1.21$ with the agreement factor $R = \Sigma(\chi_{M_{\mathrm{obs}}} - \chi_{M_{\mathrm{calcd.}}})^2/\Sigma(\chi_{M_{\mathrm{obs}}})^2 = 3.50 \times 10^{-7}$. The J value indicates that an antiferromagnetic Cu···Cu exchange interaction occurs through the bidentate bridging carboxylate groups of the NDC ligand, while the θ value indicates that the dinuclear unit presents ferromagnetic interactions through the bis(monodentate) bridging carboxylate groups of the NDC ligand.

Photoluminescent Properties

We also investigated the photoluminescent properties of compounds **3** and **4**. The emission spectra of compounds **3** and **4** in the solid state at room temperature are shown in Figure 12. It can be seen that compound **3** exhibits an intense blue photoluminescence upon photoexcitation at 386 nm. The emission peak is located at 488 nm for **3**, which means that it is bathochromically shifted by about 20 nm relative to that of the free NDC ligand, probably due to ligand-to-metal charge transfer (LMCT). The blue fluorescent emission of **3** suggests that it might be used as a new blue-light-emitting material. Compound **4** exhibits intense green photoluminescence upon photoexcitation at 380 nm. The emission peak is located at 549 nm for **4**, and compared with the NDC ligand a clearly bathochromic shift occurs in **4**, which might also be attributed to LMCT.[27–29]

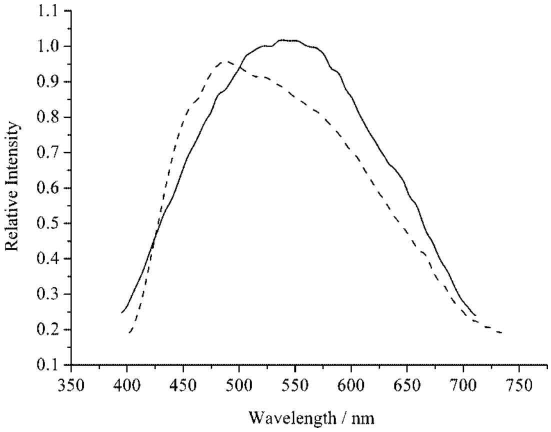

Figure 12. Emission spectra of **3** (broken line) and **4** measured in the solid state at room temperature.

Conclusions

Despite the extensive use of organic carboxylate ligands in the construction of new MOFs, combining both 2,6-naphthalenedicarboxylic acid and some other N-heteroaromatic ligands is a fairly small subset of MOFs. Four two-dimensional layer coordination compounds bridged by 2,6-naphthalenedicarboxylate and N-heteroaromatic ligands have been prepared and characterized. Substitution of metal cations or N-heteroaromatic ligands results in significant different frameworks. Compound **1** consists of three different chains that are interconnected to form an unusual two-dimensional layered motif, while compound **4** features a two-dimensional honeycomb network structure with a noninterpenetrated ABCDABCD packing pattern. Compounds **2** and **3** show a two-dimensional grid-type framework but with different space-filling styles. The magnetic studies indicate antiferromagnetic interactions transferred by the carboxylate groups of the NDC ligand in compounds **1** and **2**. Compounds **3** and **4** display strong fluorescence emission at different wavelengths.

Experimental Section

General Remarks: The syntheses were performed in Teflon-lined stainless steel autoclaves under autogenous pressure. Reagents were purchased commercially and were used without further purification. Elemental analyses of C and H were performed with an EA1110 CHNS-0 CE elemental analyzer. The IR (KBr pellet) spectra were recorded with a Nicolet Magna 750FT-IR spectrometer. TGA analyses were carried out under nitrogen at a heating rate of 10 °C min^{-1} with an STA449C integration thermal analyzer. Variable-temperature (5–300 K) magnetic susceptibility measurements were carried out with a Quantum Design MPMS-7 SQUID magnetometer at a magnetic field of 5 T using the SQUID method. The fluorescent data were collected with an Edinburgh FL-FS920 TCSPC system.

$[Cu_3(NDC)_3(2,2'\text{-bpy})(H_2O)_2]_n\cdot nH_2O$ (1): A mixture of $Cu(CH_3COO)_2\cdot H_2O$ (0.20 g, 1 mmol), NDC (0.26 g, 1 mmol), 2,2′-bpy (0.16 g, 1 mmol), and triethylamine (0.28 mL, 2 mmol) in H_2O (18 mL) was heated at 170 °C for 5 d in a sealed 30-mL Teflon-lined stainless steel vessel under autogenous pressure. Slow cooling of the reaction mixture to room temperature gave green crystals (yield: 0.19 g, 56% based on Cu). $C_{46}H_{32}Cu_3N_2O_{15}$ (1043.4): calcd. C 52.95, H 3.09, N 2.68; found C 53.13, H 2.95, N 2.54. IR (solid KBr pellet): $\tilde{\nu}$ = 3649 m, 3076 m, 1606 s, 1545 s, 1498 m, 1477 m, 1404 s, 1350 s, 1194 m, 931 w, 910 w, 843 w, 791 s, 775 s, 727 m, 650 w, 582 w, 513 w, 480 m, 447 w cm^{-1}.

$[Cu(NDC)(1,10\text{-phen})]_n$ (2): A mixture of $Cu(CH_3COO)_2\cdot H_2O$ (0.30 g, 1.5 mmol), NDC (0.13 g, 0.5 mmol), 1,10-phen (0.20 g, 1 mmol), and triethylamine (0.28 mL, 2 mmol) in H_2O (18 mL) was heated at 160 °C for 3 d in a sealed 30-mL Teflon-lined stainless steel vessel under autogenous pressure. Slow cooling of the reaction mixture to room temperature gave blue crystals (yield: 0.28 g, 62% based on Cu). $C_{24}H_{14}CuN_2O_4$ (457.93): calcd. C 62.95, H 3.08, N 6.12; found C 62.73, H 3.14, N 6.26. IR (solid KBr pellet): $\tilde{\nu}$ = 1633 s, 1616 s, 1587 s, 1518 m, 1493 m, 1425 m, 1390 s, 1350 sh, 1298 m, 1196 m, 1178 m, 1136 w, 1105 w, 937 w, 872 w, 852 s, 791 sh, 739 m, 723 s, 648 m, 577 m, 494 w, 430 w cm^{-1}.

$[Zn(NDC)(1,10\text{-phen})]_n$ (3): Compound **3** was synthesized in an analogous manner to **2** except that $Zn(CH_3COO)_2\cdot 2H_2O$ (0.22 g, 1 mmol) was used instead of $Cu(CH_3COO)_2\cdot H_2O$. The reaction mixture was cooled, which led to the formation of yellow crystals of **3** (yield: 0.24 g, 52% based on Zn). $C_{24}H_{14}N_2O_4Zn$ (459.77): calcd. C 62.70, H 3.07, N 6.09; found C 62.65, H 3.02, N 6.46. IR (solid KBr pellet): $\tilde{\nu}$ = 1628 s, 1603 m, 1556 s, 1520 m, 1495 m, 1435 s, 1421 s, 1331 s, 1296 s, 1178 m, 1132 m, 1105 w, 1047 w, 924 w, 843 m, 795 s, 768 m, 725 s, 642 w, 557 m, 540 w, 488 w, 424 w cm^{-1}.

$[Zn_4(OH)_2(NDC)_3(2,2'\text{-bpy})_2]_n$ (4): Compound **4** was synthesized in a similar manner to **3** except that 2,2′-bpy (0.16 g, 1 mmol) was used instead of 1,10-phen. The reaction mixture was cooled, which led to the formation of light yellow crystals of **4** (yield: 0.12 g, 40%

based on Zn). $C_{56}H_{36}N_4O_{14}Zn_4$ (1250.4): calcd. C 53.79, H 2.90, N 4.48; found C 53.36, H 2.68, N 4.23. IR (solid KBr pellet): $\tilde{\nu}$ = 3521 m, 3088 w, 1616 s, 1581 s, 1493 m, 1471 m, 1444 m, 1400 s, 1360 s, 1192 m, 1155 m, 1097 w, 1024 w, 924 w, 839 w, 785 s, 735 w, 667 m, 652 w, 580 w, 486 w cm^{-1}.

X-ray Crystallographic Study: Suitable single crystals with dimensions of 0.56 × 0.24 × 0.14 mm (**1**), 0.50 × 0.35 × 0.20 mm (**2**), 0.36 × 0.32 × 0.16 mm (**3**), and 0.35 × 0.25 × 0.20 mm (**4**) were glued to thin glass fibers with epoxy resin. Crystal structure measurements for compounds **1**–**4** were performed with a Rigaku Mercury CCD diffractometer with graphite-monochromated Mo-K_{α} radiation (λ = 0.71073 Å) at room temperature. A total of 3394, 4479, 3271, and 5639 unique reflections were collected by the $\omega/2\theta$ scan mode for **1**–**4**, respectively. The structures were solved by direct methods and refined on F^2 with the SHELXL-97 program.[30] All non-hydrogen atoms were refined with anisotropic displacement parameters, and the hydrogen atoms were treated as riding atoms

Table 1. Crystal data and structures refinement for compounds **1**–**4**.

	1	**2**	**3**	**4**
Empirical formula	$C_{46}H_{32}Cu_3N_2O_{15}$	$C_{24}H_{14}CuN_2O_4$	$C_{24}H_{14}N_2O_4Zn$	$C_{56}H_{36}N_4O_{14}Zn_4$
Formula mass	1043.36	457.91	459.74	1250.37
Crystal system	monoclinic	monoclinic	triclinic	monoclinic
Space group	$C2/c$	$P2_1/n$	$P\bar{1}$	$P2_1/c$
a [Å]	21.3745(6)	12.0819(11)	9.22740(10)	8.5939(5)
b [Å]	13.0065(2)	13.8007(11)	11.0681(2)	20.5943(13)
c [Å]	15.5522(2)	12.1050(10)	11.06780(10)	14.0052(11)
α [°]	90	90	119.5250(10)	90
β [°]	115.452(2)	103.563(4)	91.5900(10)	96.317(3)
γ(°)	90	90	104.6890(10)	90
V [Å^3]	3904.00(13)	1962.1(3)	935.63(2)	2463.7(3)
Z	4	4	2	2
$D_{calcd.}$ [g cm^{-3}]	1.765	1.550	1.632	1.686
$F(000)$	2116	932	468	1264
μ [mm^{-1}]	1.702	1.149	1.350	2.000
GOF	1.062	1.003	1.048	1.071
R_1, wR_2 [$I > 2\sigma(I)$][a]	0.0820, 0.1975	0.0420, 0.1251	0.0847, 0.1778	0.0427, 0.0925
R_1, wR_2 (all data)	0.1159, 0.2278	0.0504, 0.1334	0.0917, 0.1827	0.0503, 0.0968

[a] $R_1 = \Sigma(|F_o| - |F_c|)/\Sigma|F_o|$; $wR_2 = [\Sigma w(F_o{}^2 - F_c{}^2)^2/\Sigma w(F_o{}^2)^2]^{0.5}$.

Table 2. Selected bond lengths [Å] and angles [°] for compounds **1**–**4**.

Compound **1**					
Cu(1)-O(5)	1.966(5)	O(5)^{I}-Cu(1)-O(5)	89.2(3)	O(3)^{I}-Cu(2)-O(7)	87.9(2)
Cu(1)-N(1)^{I}	1.984(6)	O(5)^{I}-Cu(1)-N(1)	159.6(2)	O(1)-Cu(2)-O(7)	90.2(2)
Cu(2)-O(3)^{II}	1.932(5)	O(5)-Cu(1)-N(1)	97.7(2)	O(3)^{I}-Cu(2)-O(6)	89.9(2)
Cu(2)-O(1)	1.934(5)	O(5)-Cu(1)-N(1)^{I}	159.6(2)	O(1)-Cu(2)-O(6)	92.2(2)
Cu(2)-O(7)	1.969(6)	N(1)-Cu(1)-N(1)^{I}	82.5(4)	O(7)-Cu(2)-O(6)	176.6(2)
Cu(2)-O(6)	1.996(5)	O(3)^{II}-Cu(2)-O(1)	174.6(2)		
Compound **2**					
Cu(1)-O(2)	1.9139(18)	O(2)-Cu(1)-O(4)^{III}	95.89(8)	O(4)^{III}-Cu(1)-N(1)	166.19(8)
Cu(1)-O(4)^{III}	1.9437(16)	O(2)-Cu(1)-N(2)	170.58(8)	N(2)-Cu(1)-N(1)	80.94(8)
Cu(1)-N(2)	2.029(2)	O(4)^{III}-Cu(1)-N(2)	91.63(7)	O(2)-Cu(1)-O(3)	98.80(8)
Cu(1)-N(1)	2.050(2)	O(2)-Cu(1)-N(1)	90.52(8)	O(4)^{III}-Cu(1)-O(3)	102.41(7)
Cu(1)-O(3)	2.2421(17)				
Compound **3**					
Zn(1)-O(4)^{IV}	2.074(5)	O(4)^{IV}-Zn(1)-O(4)	79.2(2)	O(2)-Zn(1)-N(2)	90.8(2)
Zn(1)-O(4)	2.087(5)	O(4)^{IV}-Zn(1)-N(1)	97.9(2)	O(4)^{IV}-Zn(1)-O(1)	96.1(2)
Zn(1)-N(1)	2.109(6)	O(4)-Zn(1)-N(1)	97.1(2)	O(4)-Zn(1)-O(1)	155.1(2)
Zn(1)-O(2)	2.158(5)	O(4)^{IV}-Zn(1)-O(2)	95.6(2)	N(1)-Zn(1)-O(1)	107.8(2)
Zn(1)-N(2)	2.173(7)	O(4)-Zn(1)-O(2)	95.1(2)	O(2)-Zn(1)-O(1)	60.8(2)
Zn(1)-O(1)	2.177(5)	N(1)-Zn(1)-O(2)	163.3(2)	N(2)-Zn(1)-O(1)	94.3(2)
		O(4)^{IV}-Zn(1)-N(2)	169.5(2)	O(4)-Zn(1)-N(2)	92.0(2)
				N(1)-Zn(1)-N(2)	77.4(2)
Compound **4**					
Zn(1)-O(5)	1.918(2)	O(5)-Zn(1)-O(7)	132.88(11)	O(4)-Zn(2)-O(1)	93.58(13)
Zn(1)-O(7)	1.932(2)	O(5)-Zn(1)-O(3)	106.47(9)	O(5)-Zn(2)-N(2A)	127.44(19)
Zn(1)-O(3)	1.981(2)	O(7)-Zn(1)-O(3)	108.69(11)	O(4)-Zn(2)-N(2A)	89.53(18)
Zn(1)-O(2)	2.005(2)	O(5)-Zn(1)-O(2)	102.66(10)	O(1)-Zn(2)-N(2A)	133.3(2)
Zn(2)-O(5)	1.918(2)	O(7)-Zn(1)-O(2)	98.76(11)	O(5)-Zn(2)-N(1A)	116.73(17)
Zn(2)-O(4)	2.028(2)	O(3)-Zn(1)-O(2)	103.23(10)	O(4)-Zn(2)-N(1A)	141.13(17)
Zn(2)-O(1)	2.065(3)	O(5)-Zn(2)-O(4)	100.97(9)	O(1)-Zn(2)-N(1A)	73.28(18)
Zn(2)-N(2A)	2.078(5)	O(5)-Zn(2)-O(1)	97.66(10)	N(2A)-Zn(2)-N(1A)	75.5(2)
Zn(2)-N(1A)	2.203(6)				

Symmetry transformations used to generate equivalent atoms: I: $-x, y, -z + 1/2$; II: $x, y + 1, z$ for compound **1**; III: $-x, -y, -z$ for compound **2**; IV: $-x + 1, -y + 1, -z + 2$ for compound **3**.

using the SHELX-97 default parameters. For **1**, the hydrogen atoms of the water molecules were neither found nor calculated. For **4**, the 2,2′-bpy ring was found to be disordered and was modeled in two positions with occupancies of 51.2 and 48.8%. The crystal data and details of refinements for the compounds are summarized in Table 1, while their selected bond lengths and angles are listed in Table 2. CCDC-271318 (**1**), -255855 (**2**), -271317 (**3**), and -271319 (**4**) contain the supplementary crystallographic data for this paper. These data can be obtained free of charge from The Cambridge Crystallographic Data Centre via www.ccdc.cam.ac.uk/data_request/cif.

Acknowledgments

This work was supported by the 973 program of the MOST (001CB108906), the National Science Foundation of China (20425313, 90206040, 20333070, and 20303021), the NSF of Fujian, and the Chinese Academy of Sciences.

---

[1] J. S. Seo, D. H. L. Whang, S. I. Jun, J. Oh, Y. J. Jeon, K. Kim, *Nature* **2000**, *404*, 982–986.

[2] S. Noro, S. Kitagawa, M. Kondo, K. Seki, *Angew. Chem. Int. Ed.* **2000**, *39*, 2081–2084.

[3] J. Zhang, W. B. Lin, Z. F. Chen, R. G. Xiong, B. F. Abrahams, H. K. Fun, *J. Chem. Soc., Dalton Trans.* **2001**, 1806–1808.

[4] B. H. Ye, M. L. Tong, X. M. Chen, *Coord. Chem. Rev.* **2005**, *249*, 545–565.

[5] a) N. L. Rosi, J. Eckert, M. Eddaoudi, D. T. Vodak, J. Kim, M. O'Keeffe, O. M. Yaghi, *Science* **2003**, *300*, 1127–1129; b) J. Kim, B. L. Chen, T. M. Reineke, H. Li, M. Eddaoudi, D. B. Moler, M. O'Keeffe, O. M. Yaghi, *J. Am. Chem. Soc.* **2001**, *123*, 8239–8247; c) B. L. Chen, M. Eddaoudi, S. T. Hyde, M. O'Keeffe, O. M. Yaghi, *Science* **2001**, *291*, 1021–1023; d) M. Eddaoudi, J. Kim, N. Rosi, D. Vodak, J. Wachter, M. O'Keeffe, O. M. Yaghi, *Science* **2002**, *295*, 469–472; e) N. L. Rosi, M. Eddaoudi, J. Kim, M. O'Keeffe, O. M. Yaghi, *Angew. Chem. Int. Ed.* **2002**, *41*, 284–287; f) H. Li, M. Eddaoudi, M. O'Keeffe, O. M. Yaghi, *Nature* **1999**, *402*, 276–279; g) M. Eddaoudi, D. B. Moler, H. Li, B. L. Chen, T. M. Reineke, M. O'Keette, O. M. Yaghi, *Acc. Chem. Res.* **2001**, *34*, 319–330; h) N. L. Rosi, J. Kim, M. Eddaoudi, B. Chen, M. O'Keeffe, O. M. Yaghi, *J. Am. Chem. Soc.* **2005**, *127*, 1504–1518; i) D. T. Vodak, M. E. Braun, J. Kim, M. Eddaoudi, O. M. Yaghi, *Chem. Commun.* **2001**, 2534–2535.

[6] A. Filipe, P. Almeida, K. Jacek, *Chem. Commun.* **2003**, 1484–1485.

[7] S. Dalai, P. S. Mukherjee, E. Zangrando, F. Lloret, N. R. Chaudhuri, *J. Chem. Soc., Dalton Trans.* **2002**, 822–823.

[8] Z. He, E. Q. Gao, Z. M. Wang, C. H. Yan, M. Kurmoo, *Inorg. Chem.* **2005**, *44*, 862–874.

[9] B. H. Ye, B. B. Ding, Y. Q. Weng, X. M. Chen, *Cryst. Growth Des.* **2005**, *5*, 801–806.

[10] X. J. Li, R. Cao, Y. Q. Sun, W. H. Bi, X. Li, Y. Q. Wang, *Eur. J. Inorg. Chem.* **2005**, 321–329.

[11] C. Y. Su, A. M. Goforth, M. D. Smith, P. J. Pellechia, H. C. zur Loye, *J. Am. Chem. Soc.* **2004**, *126*, 3576–3586.

[12] a) T. K. Maji, G. Mostafa, H. C. Chang, S. Kitagawa, *Chem. Commun.* **2005**, 2436–2438; b) S. Furukawa, M. Ohba, S. Kitagawa, *Chem. Commun.* **2005**, 865–867; c) T. K. Maji, K. Uemura, H. C. Chang, R. Matsuda, S. Kitagawa, *Angew. Chem. Int. Ed.* **2004**, *43*, 3269–3272.

[13] B. L. Wu, D. Q. Yuan, F. L. Jiang, R. H. Wang, L. Han, Y. F. Zhou, M. C. Hong, *Eur. J. Inorg. Chem.* **2004**, 2695–2700.

[14] E. Y. Choi, Y. U. Kwon, *Inorg. Chem.* **2005**, *44*, 538–545.

[15] a) Y. B. Go, X. Q. Wang, E. V. Anokhina, A. J. Jacobson, *Inorg. Chem.* **2004**, *43*, 5360–5367; b) R. H. Groenman, L. R. MacGillivaray, J. L. Atwood, *Chem. Commun.* **1998**, 2735–2736; c) C. S. Hong, Y. Do, *Inorg. Chem.* **1998**, *37*, 4470–4472.

[16] a) X. Shi, G. Zhu, Q. Fang, G. Wu, G. Tian, R. Wang, D. Zhang, M. Xue, S. Qiu, *Eur. J. Inorg. Chem.* **2004**, 185–191; b) X. M. Zhang, M. L. Tong, M. L. Gong, X. M. Chen, *Eur. J. Inorg. Chem.* **2003**, 138–142; c) D. F. Sun, R. Cao, Y. Liang, Q. Shi, W. P. Su, M. C. Hong, *J. Chem. Soc., Dalton Trans.* **2001**, 2335–2340.

[17] a) K. O. Kongshaug, H. Fjellvag, *Solid State Sci.* **2003**, *5*, 303–310; b) K. O. Kongshaug, H. Fjellvag, *Solid State Sci.* **2002**, *4*, 443–447; c) S. W. Lee, H. J. Kim, Y. K. Lee, K. Park, J. H. Son, Y. U. Kwon, *Inorg. Chim. Acta* **2003**, *353*, 151–158.

[18] J. C. Dai, X. T. Wu, S. M. Hu, Z. Y. Fu, J. J. Zhang, W. X. Du, H. H. Zhang, R. Q. Sun, *Eur. J. Inorg. Chem.* **2004**, 2096–2106.

[19] L. Carlucci, G. Ciani, D. M. Proserpio, A. Sironi, *Angew. Chem. Int. Ed. Engl.* **1996**, *35*, 1088–1090.

[20] E. Colacio, J. M. Dominguez-Vera, F. Lloret, J. M. M. Sanchez, R. Kivekas, A. Rodriguez, R. Sillanpaa, *Inorg. Chem.* **2003**, *42*, 4209–4214.

[21] B. L. Chen, F. R. Fronczek, A. W. Maverick, *Inorg. Chem.* **2004**, *43*, 8209–8211.

[22] P. Pascal, *Ann. Chim. Phys.* **1910**, *19*, 5–7.

[23] Y. F. Song, P. Gamez, O. Roubeau, M. Lutz, A. L. Spek, J. Reeijk, *Eur. J. Inorg. Chem.* **2003**, 2924–2928.

[24] J. C. Liu, G. C. Guo, J. S. Huang, X. Z. You, *Inorg. Chem.* **2003**, *42*, 235–243.

[25] Y. Agnus, R. Louis, B. Metz, C. Boudon, J. P. Gisselbrecht, M. Gross, *Inorg. Chem.* **1991**, *30*, 3155–3161.

[26] S. Gupta, A. Mukherjee, M. Nethaji, A. R. Chakravarty, *Polyhedron* **2004**, *23*, 643–647.

[27] a) J. Tao, X. Yin, Y.-B. Jiang, L. F. Yang, R. B. Huang, L. S. Zheng, *Eur. J. Inorg. Chem.* **2003**, 2678–2682; b) J. Tao, Y. Zhang, M. L. Tong, X. M. Chen, T. Yuan, C. L. Lin, X. Y. Huang, J. Li, *Chem. Commun.* **2002**, 1342–1343.

[28] X. L. Wang, C. Qin, E. B. Wang, Y. G. Li, N. Hao, C. W. Hu, L. Xu, *Inorg. Chem.* **2004**, *43*, 1850–1856.

[29] S. L. Zheng, J. H. Yang, X. L. Yu, X. M. Chen, W. T. Wong, *Inorg. Chem.* **2004**, *43*, 830–838.

[30] G. M. Sheldrick, *SHELXS97, Program for Solution of Crystal Structures*; University of Göttingen, Göttingen, Germany, **1997**.

Received: May 31, 2005